First-passage times for pattern formation in nonlocal partial differential equations

Research · October 2015

DOI: 10.13140/RG.2.1.3175.7527

2 authors:

Manuel O Cáceres

Comisión Nacional de Energía Atómica

Miguel Angel Fuentes

National Scientific and Technical Research C…

First-passage times for pattern formation in nonlocal partial differential equations

Manuel O. Cáceres[1,*] and Miguel A. Fuentes[2,3,4]

[1] *Centro Atómico Bariloche, CNEA, Instituto Balseiro, Universidad Nacional de Cuyo, and CONICET, Avenida E. Bustillo 9500, CP 8400, Bariloche, Argentina*

[2] *Santa Fe Institute, 1399 Hyde Park Road, Santa Fe, New Mexico 87501, USA*

[3] *Instituto de Investigaciones Filosóficas, Bulnes 642, Buenos Aires 1428, Argentina*

[4] *Universidad San Sebastián, Lota 2465, Santiago 7500000, Chile*

(Received 28 May 2015; revised manuscript received 16 August 2015; published xxxxxx)

We describe the lifetimes associated with the stochastic evolution from an unstable uniform state to a patterned one when the time evolution of the field is controlled by a nonlocal Fisher equation. A small noise is added to the evolution equation to define the lifetimes and to calculate the mean first-passage time of the stochastic field through a given threshold value, before the patterned steady state is reached. In order to obtain analytical results we introduce a stochastic multiscale perturbation expansion. This multiscale expansion can also be used to tackle multiplicative stochastic partial differential equations. A critical slowing down is predicted for the marginal case when the Fourier phase of the unstable initial condition is null. We carry out Monte Carlo simulations to show the agreement with our theoretical predictions. Analytic results for the bifurcation point and asymptotic analysis of traveling wave-front solutions are included to get insight into the noise-induced transition phenomena mediated by invading fronts.

DOI: 10.1103/PhysRevE.00.002100 PACS number(s): 05.40.−a, 82.40.Ck, 87.18.Hf

I. INTRODUCTION

Nonlinear systems out of equilibrium exhibit a variety of instabilities when the appropriate control parameters are changed. By such changes of control parameters the system can be placed in a stationary state that is not globally stable. One phenomenon in which statistical fluctuations play a crucial role in nonequilibrium descriptions is the transient dynamics associated with the relaxation from states that have lost their global stability due to changes of the appropriate control parameters. A quantity in the characterization of the relaxation dynamics is the lifetime of such states, i.e., the random time that the system takes to leave the vicinity of the initial state. The statistics of these times is described by the first-passage-time distribution (FPTD) and the mean first-passage time (MFPT) is identified by the lifetime of the initial state. There are standard techniques [1] to calculate the MFPT for Markov processes; a useful alternative route to these techniques focuses on the individual stochastic path of the process and extract the FPTD from approximations of these paths [2,3]. This stochastic path perturbation approach can also be generalized to tackle non-Markov processes [4], non-Gaussian noises [5], and stochastic differential equations with distributed time delay [6]. From a practical point of view, the stochastic path perturbation approach is useful in the calculation of the MFPT in situations in which standard techniques do not hold straightforwardly, such as in extended dynamically systems [7] and in the analysis of the MFPT in stochastic partial integro-differential equations (nonlocal models) [8,9].

In the past 20 years there has been much interest in the study of nonlocal models in ecology and biology. Most of them have been formulated in terms of continuous-field evolution equations for densities describing long-distance interactions [10,11]. These interactions can be mediated through vision, hearing, smelling or other kinds of sensing. Therefore, nonlocal effects in nonlinear terms in reaction-diffusion equations may account for the resource's competition within a certain range. It is worth mentioning studies of bacteria cultures in Petri dishes in which the diffusion of nutrients and/or the release of toxic substances can cause nonlocality in the interactions [12–15]. Moreover, we can mention related works such as the study of traveling-wave solutions of nonlocal reaction-diffusion equations arising also in population dynamics [16]. Other studies refer to the pattern formation phenomena in a model of competing populations with nonlocal interactions [17]. Very recently, plant clonal morphologies and spatial patterns were modeled with nonlocal linear and nonlinear terms in extended systems [18]. Nonlocal dynamics have also been used in nonlinear optics where the space-time evolution of the intracavity field was described by the Lugiano-Lefever model with nonlocal interactions [19]. There are also several works related to neural fields, where nonlocal interactions and noise-induced jumps play an important role in the description of real systems [20,21]. In this paper we focus on the study of the MFPT for a stochastic nonlocal version of the so-called Lotka-Volterra, or Fisher, equation [11,22,23] (due to environmental or thermic fluctuation acting on these types of systems, we include an additive noise in the evolution equation of the field). We are especially concerned with the description of the lifetime of the system (due to the change of stability) from a uniform state to a patterned stationary state near criticality.

Depending on the physical parameters of the system, new scenarios may appear; for example, if the value of the diffusion coefficient changes, the stability of the homogeneous state may change because a Fourier vector k_e may become unstable. In particular, the situation when the phase of the Fourier mode vanishes $\varphi(k_e) = 0$, for a given value of Fourier wave vector k_e, may happen, leading therefore to a critical slowing down of the escape process (lifetime of the unstable state). The

*Corresponding author: caceres@cab.cnea.gov.ar

supercritical case $\varphi(k_e) > 0$ was analyzed very recently [8,9], but the critical case is much more complex to work out because the instability turns out to be nonlinear. On the other hand, the essential difficulty describing the relaxation from a state of marginal stability [i.e., when $\varphi(k_e) = 0$] is that there is no regime in which a linear approximation is meaningful. These issues will be resolved in the present work by introducing a stochastic multiple-scale expansion, with the application of the stochastic path perturbation approach.

A related work describing a stochastic supercritical bifurcation for local partial differential equations was presented recently [24]. In that paper a multiscale perturbation was proposed to build a stochastic ordinary differential equation. After solving the stationary Fokker-Planck equation for the amplitude of the most unstable mode, the influence of the noise on the shape of the imperfect supercritical bifurcation was characterized by the most probable amplitude. It could be very interesting to generalize that approach to the case of nonlocal partial differential equations like the one we propose to work out in the present paper.

In Sec. II we show the mathematical model that we use. In Sec. III we study the bifurcation point and present a deterministic asymptotic wave-front analysis. In Sec. IV we perform the discrete Fourier analysis to study the stochastic model in a finite domain, In Sec. V we introduce a minimum coupling approximation to tackle the nonlocality of the model with an approximation. In Sec. VI we introduce the stochastic multiscale perturbation expansion, derive the MFPT using the stochastic path perturbation approach, and then compare our results with numerical simulations. In Sec. VII we present a summary and possible extensions of the program. Extended calculations related to the present work are given in the Appendixes.

II. STOCHASTIC NONLOCAL FISHER EQUATION

The dynamical model, shown in Eq. (1), takes into account the exponential growth of the population, characterized by the parameter a, a diffusion constant D, a nonlocal competition term proportional to a parameter b, and the interaction kernel $G(x)$. We also model environmental or thermic fluctuations acting on these types of systems. To take this into account we introduce an additive fluctuating Gaussian field $\xi(x,t)$ in the dynamics. This is a plausible ansatz when the unspecified random contributions are more important at low density (see Appendix 3 in [6]). We characterize the strength of the noise with a small parameter ϵ.

The one-dimensional model takes the form

$$\frac{\partial u(x,t)}{\partial t} = D\frac{\partial^2 u(x,t)}{\partial x^2} + au(x,t) - bu(x,t) \times \int_{-L}^{L} u(x-x',t)G(x')dx' + \sqrt{\epsilon}\xi(x,t). \quad (1)$$

We are interested in the stochastic pattern formation description of the (positive) density field $u(x,t)$ of Eq. (1), subject to periodic boundary conditions in $[-L,L]$. The random characteristics of this stochastic integro-differential equation are completely characterized by the statistics of the field $\xi(x,t)$. Nevertheless, the first-passage-time problem associated with this model is nontrivial due to the characteristics introduced by the nonlocal term contribution. In the present study we use Gaussian white-noise moments [1,25,26]

$$\langle \xi(x,t)\rangle = 0, \quad \langle \xi(x,t)\xi(x',t')\rangle = \delta(x-x')\delta(t-t').$$

The nonlocal interaction, i.e., the kernel $G(x)$, is adopted to be symmetric and normalized in the domain of interest $[-L,L]$. We use a square kernel defined as

$$G(x) = \frac{1}{2w}[\Theta(w-x)\Theta(w+x)], \quad (2)$$

where the step function $\Theta(x) = 0$ if $x < 0$ and $\Theta(x) = 1$ if $x > 0$. Thus the limit $w \to 0$ reproduces a local interaction and the limit $w \to L$ represents a nonlocal interaction in the complete domain $[-L,L]$. In [13] several types of kernels and their analytical properties were presented.

The deterministic version of the model, Eq. (1) with $\epsilon = 0$, has two homogeneous steady states u_{SS}: $\{0,a/b\}$. In the local case those values constitute the unstable and stable fixed points, respectively; note that the nonlocal Fisher model is nonvariational. For the nonlocal case we are interested mainly in the instability that occurs with the fully populated state, i.e., $u_{SS} = a/b$. This instability can be understood by doing a linear analysis around u_{SS} [see Eq. (22)] and its appearance depends on the growth parameter a, the diffusion constant D, and the Fourier transformation of the nonlocal interaction kernel $G(x)$; these characteristics are analyzed in detail in the following sections. Then, for a given set of parameters [see Eq. (23)], the uniform initial condition u_{SS} becomes unstable, so, due to fluctuations, the dynamics end in a patterned stable solution.

We show in Fig. 1 a realization of the stochastic dynamics [Eq. (1)] in the course of time. In addition, in Fig. 2 we also show the evolution of a pure deterministic solution. This figure shows the attractor of the system and the evolution to reach it from the patterned initial condition $u(x,0) = 1.0 + 0.85\cos(2\pi x)$. This graph shows four times $t = 0,20,50,150$ for the deterministic evolution of $u(x,t)$ [Eq. (1) with $\epsilon = 0$]. As can be seen, the attractor is almost reached (from this

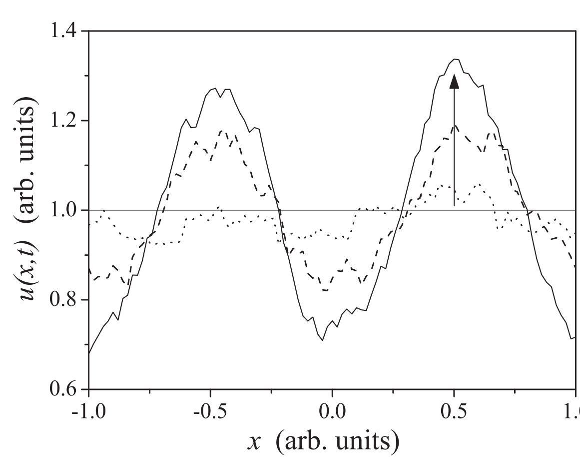

FIG. 1. Typical stochastic evolution of the field $u(x,t)$. The initial condition is $u(x,0) \equiv u_{SS} = 1$ and the evolution follows Eq. (1) with $\epsilon = 10^{-2}$. The physical parameters a,b,D,w,L are chosen in such a way that the initial condition is marginally unstable (see Tables I and II). The arrow shows the amplitude of the stochastic evolution of Fisher's field at three different times $t = 50,75,150$, i.e., evolving from the uniform toward the patterned state.

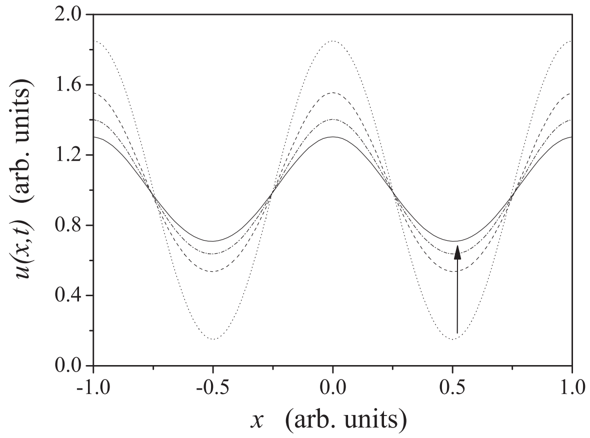

FIG. 2. Typical deterministic evolution of the field $u(x,t)$. The initial condition $u(x,0) = 1.0 + 0.85\cos(2\pi x)$ follows the time evolution of Eq. (1) with $\epsilon = 0$. The physical parameters a,b,D,w,L are the same as in Fig. 1 (see Tables I and II). The arrow shows the evolution of the amplitude at three different times $t = 20,50,150$, showing the approach to the patterned final steady state.

deterministic evolution) at a time around $t = 150$. Therefore, an important point in the description of the pattern formation is to investigate its transient stochastic dynamics from the stationary uniform initial condition to the final inhomogeneous solution. Figure 3 shows the typical histogram of the escape times when considering the full dynamics with the addition of noise (1). Not only is the MFPT an important quantity to be known; also the possible existence of a long-time tail in the FPTD will be investigated in the present paper. In the following sections we will be interested in the analytical description of the MFPT. To do this we introduce a multiscale perturbation expansion and use the stochastic path perturbation approach to tackle the escape times from a marginal unstable state evolved from Eq. (1).

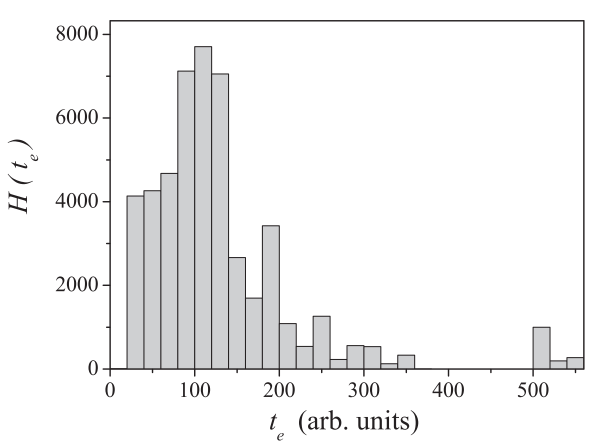

FIG. 3. Histogram of the escape times from Eq. (1) for 5×10^4 realizations, using the parameters a,b,D,w,L from Tables I and II and noise intensity $\epsilon = 10^{-2}$. The random escape time t_e is considered here when the evolution of the stochastic field $u(x,t)$ reaches, for the first time, a given threshold value, i.e., $\Delta u \equiv [u(x,t_e)_{\max} - u(x,t_e)_{\min}]/2 = 0.275$ (see Appendix B).

III. DETERMINISTIC ANALYSIS

Before going into the stochastic problem, let us introduce a deterministic analysis associated with the nonlocal Fisher model (1), but for an infinite domain $L \to \infty$. This analysis will help in the understanding of the bifurcation condition and to get insight into the noise-induced transition phenomena mediated by invading fronts.

A. Bifurcation diagram

The dynamics close to homogeneous stationary states $u_{\rm SS}$ show that spatial instability can set in when the system parameters are changed. For example, in the next section we show the dispersion relation associated with the stationary state $u_{\rm SS} = a/b$ (see Fig. 4). This result is obtained by invoking a discrete Fourier analysis and using periodic boundary conditions in a finite domain $L < \infty$.

In this section we present a continuous Fourier analysis in order to find the bifurcation condition in the space of the parameters of our problem. From Eq. (1) the linear dynamics close to $u_{\rm SS} = 0$, the unpopulated state, is

$$\partial_t \delta u = \partial_x^2 \delta u + a\delta u, \tag{3}$$

while close to $u_{\rm SS} = a/b$, the fully populated state, it is

$$\partial_t \delta u = \partial_x^2 \delta u - a \int_{-\infty}^{+\infty} \delta u(x - x',t) G(x') dx'. \tag{4}$$

To obtain the spectrum (dispersion relation) we take $\delta u(x,t) \propto e^{\varphi t + ikx}$ and substitute it in the time evolution equations above to get the relation between the wave number k and φ. We find that the spectrum near the unpopulated state is

$$\varphi(k) = -Dk^2 + a \tag{5}$$

and near the fully populated state is

$$\varphi(k) = -Dk^2 - aG(k), \quad G(k) = \frac{\sin kw}{kw}. \tag{6}$$

In the present work we will be interested in the instability near the fully populated state $u_{\rm SS} = a/b$ (which sets in by the nonlocal interaction). This instability is characterized by the Fourier transform of the nonlocal kernel (2), i.e., $G(k) = \int_{-\infty}^{+\infty} e^{-ikx} G(x) dx = \frac{\sin kw}{kw}$. In order to find when the fully populated state is stable or unstable, we solve the bifurcation conditions

$$\varphi(k_c) = 0, \quad d\varphi(k_c)/dk = 0. \tag{7}$$

From these conditions we can obtain the bifurcation portrait. From Eqs. (6) and (7) we have the explicit expression for the point of bifurcation when changing the range of the interaction w (see Appendix A),

$$w_{\min}^2 = \frac{-3D\kappa}{a\cos\kappa}, \quad \kappa = 3\tan\kappa. \tag{8}$$

Therefore, by increasing the value of the nonlocal interaction range w, the fully populated state turns out to be spatially unstable. The fully populated state is spatially stable when $w < w_{\min}$ and at the critical value $w = w_{\min}$ the function $\varphi(k)$ has a maximum at k_c [i.e., $\varphi(k_c) = 0$]; when $w > w_{\min}$ the fully populated state is spatially unstable for a finite domain of k ($\varphi > 0$) (see also Sec. IV and Fig. 4). Note that in Eq. (8)

the value of the constant is $\kappa = 4.078\ldots$ (in the domain of interest) and so $\cos\kappa < 0$.

B. Wave-front solutions in the nonlocal model

Traveling-wave-front and monotonic solutions $U(z)$ for local Fisher equation exist, with $U(-\infty) = 1$ and $U(\infty) = 0$, for all wave speeds $c \geqslant 2$ (in nondimensional units). Unfortunately, no analytical solutions for the phase-plane trajectories have been found for general $c \geqslant 2$, although there is an exact solution for a particular value of c (see [11]). For the nonlocal Fisher model the situation is even more complex. Nevertheless, we can do an asymptotic analysis for a small nonlocal range $w \to 0$. This analysis helps in the understanding of the complexity of the stochastic problem that we want to solve in the present paper.

Let us consider the deterministic part of Eq. (1) in an infinite domain $L \to \infty$. It is convenient at the outset to rescale Eq. (1) by writing [note that $\int_{-\infty}^{\infty} G(x)dx = 1$]

$$u \to u \Big/ \left(\frac{a}{b}\right), \quad t \to at, \quad x \to x\sqrt{\frac{a}{D}}, \quad G \to \sqrt{\frac{D}{a}}. \tag{9}$$

Then our nonlocal Fisher model becomes

$$\frac{\partial u(x,t)}{\partial t} = \frac{\partial^2 u(x,t)}{\partial x^2} + u(x,t)\left(1 - \int_{-\infty}^{\infty} u(x-x',t)G(x')dx'\right). \tag{10}$$

In the spatially homogeneous situation the steady states are now $u_{\rm SS} = 0$ and $u_{\rm SS} = 1$. This suggests that we can look for traveling-wave-front solutions of Eq. (10) for which $0 \leqslant u \leqslant 1$. If a traveling-wave solution exists it can be written in the form $u(x,t) = U(z)$ and $z = x - ct$, where c is the wave speed to be specified; we assume $c \geqslant 0$. Upon substituting this wave front into Eq. (10), $U(z)$ satisfies

$$cU' + U'' + U\left(1 - \int_{-\infty}^{\infty} U(z-z')G(z')dz'\right) = 0, \tag{11}$$

where primes denote differentiation with respect to z. A typical front is where U at one end, say, as $z \to -\infty$, is at one steady state and as $z \to \infty$ it is at the other. So we should solve the integro-differential eigenvalue problem (11) to find the values of c such that a non-negative solution $U(z)$ exists that satisfies

$$U(z \to \infty) = 0, \quad U(z \to -\infty) = 1.$$

This is a highly difficult task, which can be worked out asymptotically, as we show next.

As we commented before, in the limit $w \to 0$ our model turns out to be local; therefore, we can use w as a small parameter to study asymptotically the front analysis. When $w \ll 1$ the integral in Eq. (10) can be approximated by

$$\int_{-\infty}^{\infty} u(x-x',t)G(x')dx' \to \sum_{n=0}^{\infty} \frac{1}{(2n)!}\frac{w^{2n}}{2n+1}\partial_x^{2n} u(x). \tag{12}$$

If the sum converges, we use the symmetry $G(x) = G(-x)$ and normalization of the density $G(x)$. Therefore, Eq. (11) can be written as

$$cU' + U'' + U\left[1 - \left(U + \frac{w^2}{6}U'' + O(w^4)\right)\right] = 0. \tag{13}$$

Introducing the variable $V = U'$ in Eq. (13), we can study, up to $O(w^2)$, this equation in the (V,U) phase plane, where

$$V' = -[cV + U(1-U)]\left(1 - \frac{w^2}{6}U\right)^{-1}, \qquad U' = V. \tag{14}$$

This system of equations is valid if $|V'w^2/6| \ll U$. If this condition is fulfilled the phase-plane trajectories are solutions of

$$\frac{dV}{dU} = \frac{-[cV + U(1-U)]}{V[1-(w^2/6)U]}. \tag{15}$$

This system has two singular points for (V,U), namely, (0,0) and (0,1). A linear stability analysis shows that the eigenvalues λ for the singular points are, for points (0,0) and (0,1), respectively,

$$\lambda_\pm = \tfrac{1}{2}[-c \pm (c^2-4)^{1/2}] \Rightarrow \begin{cases} \text{stable node if } c^2 > 4 \\ \text{degenerate node if } c^2 = 4 \\ \text{stable spiral if } c^2 < 4, \end{cases} \tag{16}$$

$$\lambda_\pm = \frac{1}{2}\left\{-\left(c + \frac{w^2 c}{6}\right) \pm \left[\left(c + \frac{w^2 c}{6}\right)^2 + 4\left(1 + \frac{w^2}{6}\right)\right]^{1/2}\right\} \Rightarrow \text{saddle point}. \tag{17}$$

Thus up to $O(w^2)$, these results show that there can be trajectories from (0,1) to (0,0) lying entirely in the quadrant $U \geqslant 0$, therefore precluding traveling-wave solutions if $c \geqslant 2\sqrt{aD}$ (in the original dimensional variables). So up to this perturbation $O(w^2)$, the slowest transition wave propagation $c_{\rm min}$ is independent of the nonlocal range w. However, as it is well known, the solution of the front depends critically on the behavior of the support of $u(x,t=0)$ (see [27]). If we wish to consider larger values of the nonlocal range w we should include the next correction $O(w^4)$ in Eq. (13); however, the difficulty in working with the next correction is that a larger phase-space dimension would be required to study the dynamical system.

The expression (17) is an acceptable solution for $w \ll \sqrt{6}\sqrt{D/a}$ (in dimensional variables). For the parameters that we have used to run the stochastic realizations this would mean $w \ll 0.181$ (see Table I). On the other hand, we know from

TABLE I. Parameters used in the present work.

Physical parameters	Description
$a = 1$	linear growth rate
$b = 1$	nonlinear coupling parameter
$D = 5.47733 \times 10^{-3}$	diffusion coefficient
$L = 1$	macroscopic size system
$w = 0.7$	cutoff in the nonlocal interaction range

the bifurcation point for $u_{SS} = a/b$ [see Eq. (8)] that in order to reach the bifurcation, a minimum value for the range of interaction $w_{\min}$ would be required, which makes the previous asymptotic analysis more difficult to implement.

Another alternative to tackling the analysis of front propagation in nonlocal Fisher models is to use a different kernel $G(x)$ in Eq. (10). In particular, if we use the Laplace probability density function (PDF) (with mean value w) we can reduce the integro-differential Fisher model to a pure differential system of higher dimension. This is possible because the Laplace PDF is the Green's function of the operator $\partial_{xx} - w^{-2}$ [6,15,28]; however, this approach is beyond the scope of the present paper.

In the present paper we use a square nonlocal kernel $G(x)$ and the problem that we want to solve is the stochastic emergence of a patterned solution from the unstable homogeneous state $u_{SS} = a/b$, which would correspond to the invading wave front from a nonmonotonic solution. This is a key question, but a mathematically difficult issue. Thus we propose to tackle this problem from the triggered-noise analysis of the random times to leave the unstable stationary state $u_{SS} = a/b$ to reach a patterned final state [in Fig. 1 we have plotted the system at the bifurcation point and used the initial condition $u(x,t=0) = a/b$]. This approach corresponds to the study of the first-passage-time distribution for an extended system, which is also a very difficult task. Nevertheless, by introducing a discrete Fourier analysis we can select the dominant unstable Fourier mode k_e (with amplitude A_e) and so we can study the first-passage time associated with the noise-induced transition from the homogeneous mode to the unstable mode k_e. This is the program of the present work. In order to carry out all these calculations, in the next section we introduce a discrete Fourier transform in Eq. (1), which is associated with the analysis of a finite domain $L < \infty$ with a suitable boundary condition.

IV. FOURIER ANALYSIS

As mentioned, in the present analysis we assume periodic boundary conditions in the interval $[-1,1]$, i.e., we use a domain size $L = 1$. In order to study the transition from a uniform stationary state to a patterned one, we decompose Eq. (1) using a discrete Fourier transformation as follows:

$$u(x,t) = \sum_{n=-\infty}^{\infty} A_n(t)\exp(ik_n x),$$

$$\xi(x,t) = \sum_{n=-\infty}^{\infty} \xi_n(t)\exp(ik_n x),$$

$$G(x) = \sum_{n=-\infty}^{\infty} G_n \exp(ik_n x),$$

where $k_n = n\pi$, $n = 0, \pm1, \pm2, \pm3, \ldots$, and $G_n = \int_{-1}^{1} G(x) \exp(-ik_n x)\frac{dx}{2} = \frac{1}{2}\frac{\sin k_n w}{k_n w}$, etc. Noting that $\int_{-1}^{1} G(x)dx = 1$, we get $G_0 = \frac{1}{2}$ and $|G_n| \leqslant 1$. Introducing these series into Eq. (1) and using that

$$\int_{-1}^{1} e^{i(m+n)\pi x}dx = 2\delta_{m+n,0}, \tag{18}$$

we arrive at

$$\begin{aligned}\partial_t \sum_{n=-\infty}^{\infty} A_n(t)e^{ik_n x} &= \sum_{n=-\infty}^{\infty} [D(ik_n)^2 + a]A_n(t)e^{ik_n x} \\ &\quad - 2b\left(\sum_{m=-\infty}^{\infty} A_m(t)e^{ik_m x}\right)\left(\sum_{n=-\infty}^{\infty} G_n A_n(t)e^{ik_n x}\right) \\ &\quad + \sqrt{\epsilon}\sum_{n=-\infty}^{\infty} \xi_n(t)e^{ik_n x}.\end{aligned}$$

Then, using the orthogonality of the Fourier series, we can write the infinite set of coupled Fourier modes

$$\frac{dA_n}{dt} = (-Dk_n^2 + a)A_n - 2b\sum_{l=-\infty}^{l=\infty} A_{n-l}A_l G_l + \sqrt{\epsilon}\xi_n(t),$$
$$\langle \xi_m(t')\xi_n(t)\rangle = \delta_{m+n,0}\,\delta(t-t'). \tag{19}$$

Introducing the usual linear stability analysis $u = u_{SS} + u_1$ with $u_{SS} = a/b$ and $u_1 = e^{\varphi t}(\sum_{n=-\infty}^{\infty} A_n e^{ik_n x})$ into the deterministic part of Eq. (1), we get

$$\partial_t u_1 = D\partial_x^2 u_1 + au_1 - bu_1 u_{SS} - bu_{SS}\int_{-1}^{1} u_1(x-x',t)G(x')dx' \tag{20}$$

$$= D\partial_x^2 u_1 + au_1 - bu_1 u_{SS} - 2bu_{SS}\left(\sum_{n=-\infty}^{\infty} G_n A_n e^{\varphi t}e^{ik_n x}\right). \tag{21}$$

Therefore, the homogeneous state $u_{SS} = a/b$ is unstable under small perturbations of the form

$$u(x,t) = a/b + e^{\varphi t + ik_n x} \tag{22}$$

if

$$\varphi = -Dk_n^2 - 2aG_n \geqslant 0. \tag{23}$$

For the particular kernel we use in the present work (2), the dispersion relation $\varphi \equiv \varphi(k_n)$ is shown in Fig. 4. Note that any typical length scale characterizing an abrupt condition for the kernel $G(x)$ (cut off in the range of nonlocal interaction) appears in the final expression of the Fourier transformation G_n. As discussed in detail in [13], an interesting characteristic of this nonlocal dynamics is the appearance of a nontrivial unstable mode, as illustrated in Fig. 1. In Tables I and II we show the corresponding numerical values of the parameters that we use in the present work.

TABLE II. Critical parameters used in the present work.

Physical parameters	Description
$G_2 = \frac{1}{2}\frac{\sin 2\pi w}{2\pi w}$	Fourier mode of the square nonlocal kernel
$\varphi = -D(2\pi)^2 - 2aG_2 = 0$	phase at the critical case using data from Table I

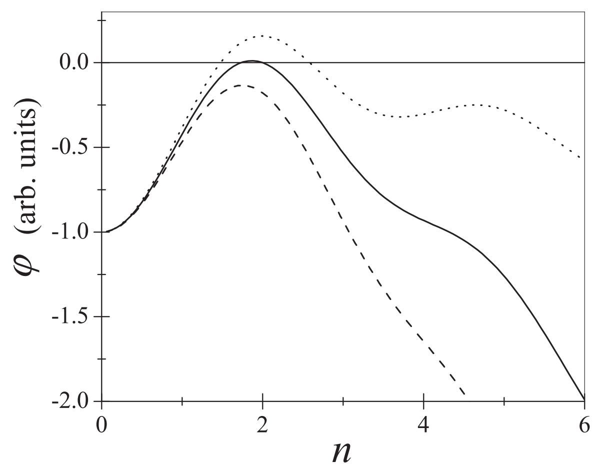

FIG. 4. Dispersion relation φ as a function of n. Equation (23) is plotted for the parameter values shown in Tables I (solid line). Note that the supercritical unstable mode in this case corresponds to $n = 2$. The dashed line is the result using the same set of parameters but with the diffusion parameter $D = 0.01$. For the dashed line, the uniform state $u_{SS} = a/b$ is stable. The dotted line is the result of using the same set of parameters but with a lower diffusion parameter $D = 0.0015$.

Therefore, depending on the physical parameters of the system, new scenarios may appear; for example, if the value of the diffusion coefficient changes (due to external agents) the stability of the homogeneous state $u_{SS} = a/b$ may change [see Eq. (23) and Fig. 4]. In particular, the situation when $\varphi(k_e) = 0$ for a given value of k_e may happen, leading therefore to a critical slowing down of the escape process. This critical case is much more complex to analyze because the instability turns out to be nonlinear; then there is no regime in which a linear approximation is meaningful. (See also the next section where we discuss the multiple-scale dynamics of the nonlocal Fisher model in terms of a minimum coupling approximation.)

V. MINIMUM COUPLING APPROXIMATION

The relations shown in Eq. (19) are the complete set of equations for the evolution of the amplitudes of all modes in the nonlocal problem given by Eq. (1). Solving this set of equations would be a difficult numerical undertaking. To make further progress analytically, we consider the situation near criticality (the onset of the pattern from a homogeneous background). Then we follow standard procedures to derive the expression for the evolution of a *single* amplitude, say, $A_e(t)$, for which $\varphi \geqslant 0$ (i.e., for the most unstable Fourier mode k_e). In this context the approximation consists in assuming that the rest of the amplitudes remain smaller than the unstable amplitude during all the time previous to the explosion of $A_e(t)$. Therefore, we only write a couple of equations for the unstable and the homogeneous modes.

When there is only one unstable Fourier wave number k_e the deterministic part of the set of equations (19) can be written in a less complex way by separating the dynamics of the homogeneous and the unstable modes

$$\frac{dA_0}{dt} = (a - bA_0)A_0 - 2b\left(A_eA_{-e}G_e + A_eA_{-e}G_{-e} + \sum_{j\neq 0,\pm e} A_jA_{-j}G_j\right), \tag{24}$$

$$\frac{dA_e}{dt} = [a(e) - bA_0(1 + 2G_e)]A_e - 2b\sum_{j\neq 0,e} A_{e-j}A_jG_j, \tag{25}$$

$$\frac{dA_{-e}}{dt} = [a(-e) - bA_0(1 + 2G_{-e})]A_{-e} - 2b\sum_{j\neq 0,-e} A_{-e-j}A_jG_j. \tag{26}$$

In the symmetrical case, i.e., when $G_e = G_{-e}$ and noting that $a(e) = a(-e) = (-Dk_e^2 + a)$ from Eqs. (24)–(26), we can prove that $A_e(t) = A_{-e}(t)$; therefore we could restrict the Fourier analysis to the case $n \geqslant 0$, which is equivalent to considering the dynamics of the modes in the form

$$\frac{dA_0}{dt} = (a - bA_0)A_0 - 2b\big[\tilde{A}_e^2G_e + X_e\big], \quad A_0(t=0)\sim O(1), \tag{27}$$

$$\frac{d\tilde{A}_e}{dt} = [a(e) - bA_0(1 + 2G_e)]\tilde{A}_e - 2b\,Y_e, \quad \tilde{A}_e(t=0)\sim 0, \tag{28}$$

where [with $\tilde{A}_e(t) = \sqrt{2}A_e(t)$]

$$X_e \equiv \sum_{j>0,\ j\neq e} 2A_l^2G_j \geqslant 0, \tag{29}$$

$$Y_e \equiv \sqrt{2}\sum_{j\neq\{0,e\}} A_{e-j}A_jG_j. \tag{30}$$

In accord with our previous assumptions [$|A_j(t)| \ll |A_e(t)|$, $j \neq 0,e$], neglecting in Eqs. (27) and (28) contributions from X_e and Y_e gives the minimum coupling approximation (MCA) [13]. Thus considering that $O(X_e)$ and $O(Y_e)$ are small perturbations to the dynamics of $A_0(t)$ and $\tilde{A}_e(t)$, the stationary states of Eqs. (27) and (28) are characterized by the equations

$$0 = (a - bA_0)A_0 - 2b\tilde{A}_e^2G_e, \tag{31}$$

$$0 = a(e) - bA_0(1 + 2G_e); \tag{32}$$

then their solutions are

$$A_0(\infty) = \frac{-Dk_e^2 + a}{b(1 + 2G_e)}, \tag{33}$$

$$\tilde{A}_e^2(\infty) = \frac{(a - bA_0)A_0}{2bG_e} = \frac{|1 - Dk_e^2/a|\varphi}{2(b^2/a)|G_e|(1 + 2G_e)^2}. \tag{34}$$

Therefore, from the MCA it is simple to see that for the critical case, when $\varphi = (-Dk_e^2 + 2a|G_e|) = 0$, the stationary solutions are given by

$$\lim_{\varphi\to 0} A_0(\infty) \to a/b, \tag{35}$$

$$\lim_{\varphi\to 0} \tilde{A}_e(\infty) \to 0. \tag{36}$$

This means that the MCA cannot be used to predict a value for the stationary state $\tilde{A}_e(\infty)$ when $\varphi \to 0$; only by going beyond the MCA is it possible to find a value $\tilde{A}_e(\infty) \neq 0$ for the critical case (see Appendix B). The growth of the explosive mode is independent of the asymptotic value $\tilde{A}_e(\infty)$, therefore we can calculate the MFPT using this approach. This means that the MCA can still be used to study the stochastic growth of the explosive amplitude $\tilde{A}_e(t)$ for the critical case.

In Appendix C we present a generalization of the MCA in the case when there are two unstable amplitudes $A_u(t), A_e(t)$. In this case the MCA gives a higher dimension set of coupled equations for the dominant modes.

VI. STOCHASTIC MULTISCALE PERTURBATION APPROACH

By neglecting $O(X_e)$ and $O(Y_e)$ in Eqs. (27) and (28), simplifying the notation $\tilde{A}_e \to A_e$, and defining the auxiliary functions $F(A_0,A_e) \equiv (a - bA_0)A_0 - 2bA_e^2 G_e$ and $Q(A_0,A_e) \equiv [a(e) - bA_0(1+2G_e)]A_e$, we can rewrite the stochastic versions of Eqs. (27) and (28) in a compact form

$$\frac{dA_0}{dt} = F(A_0,A_e) + \sqrt{\epsilon}\xi_0(t), \tag{37}$$

$$\frac{dA_e}{dt} = Q(A_0,A_e) + \sqrt{\epsilon}\xi_e(t). \tag{38}$$

Here, as commented before, $\xi_0(t)$ is statistically independent from $\xi_e(t)$. If the noise intensity ϵ is a small parameter we can introduce a multiscale perturbation expansion for the homogeneous mode $A_0(t)$ and the unstable mode $A_e(t)$ in the form

$$A_0(t) = A_0^{(0)} + \sqrt{\epsilon}x(t) + \epsilon y(t) + \epsilon^{3/2}h(t) + \cdots, \tag{39}$$

$$A_e(t) = \sqrt{\epsilon}W(t) + \epsilon V(t) + \epsilon^{3/2}J(t) + \cdots. \tag{40}$$

Introducing Eqs. (39) and (40) into Eqs. (37) and (38) and collecting different orders in ϵ, we obtain the multiple-scale dynamics. For example, for the homogeneous mode $A_0(t)$, up to $O(\epsilon^{3/2})$, we get

$$O(\epsilon^0) \Rightarrow A_0^{(0)} = a/b, \tag{41}$$

$$O(\epsilon^{1/2}) \Rightarrow \frac{dx}{dt} = -ax(t) + \xi_0(t), \tag{42}$$

$$O(\epsilon^1) \Rightarrow \frac{dy}{dt} = -ay(t) - bx(t)^2 - 2bG_eW(t)^2, \tag{43}$$

$$O(\epsilon^{3/2}) \Rightarrow \frac{dh}{dt} = -ah(t) - 2bx(t)y(t) - 4bG_eW(t)V(t). \tag{44}$$

For the dynamics of the unstable mode $A_e(t)$ we get

$$O(\epsilon^{1/2}) \Rightarrow \frac{dW}{dt} = \left(-Dk_e^2 + 2a|G_e|\right)W(t) + \xi_e(t), \tag{45}$$

$$O(\epsilon^1) \Rightarrow \frac{dV}{dt} = \left(-Dk_e^2 + 2a|G_e|\right)V(t) - b(1+2G_e)W(t)x(t), \tag{46}$$

$$O(\epsilon^{3/2}) \Rightarrow \frac{dJ}{dt} = \left(-Dk_e^2 + 2a|G_e|\right)J(t) - b(1+2G_e)[W(t)y(t) + V(t)x(t)]. \tag{47}$$

The multiscale expansion allow us to study by perturbations the stochastic escape process from any unstable state characterized by a set of equations like in (37) and (38).

A. Stochastic escape in the supercritical case $\varphi > 0$

In the small noise approximation the stochastic path perturbation approach consists of obtaining information about the first-passage-time statistics without solving the Fokker-Planck equation. This is done by analyzing the stochastic realizations of the process under study when they are written in terms of Wiener paths.

The supercritical case occurs when the phase factor $\varphi = (-Dk_e^2 + 2a|G_e|) > 0$. Therefore, the escape process of the unstable mode $A_e(t)$ is dominated by $O(\epsilon^{1/2})$, i.e., the linear stochastic differential equation (45). Consistently, the homogeneous mode is well described by Eqs. (41) and (42). Due to the linearity of the unstable evolution, the stochastic path perturbation approach can easily be introduced by working out the Wiener realization up to $O(\epsilon^{1/2})$ [5], for this linear unstable case and in the small noise approximation the first-passage-time statistics are independent of the saturation of the unstable mode [29], i.e., the steady states (33) and (34).

In the supercritical case we can interpret the multiscale dynamics in the following form: To $O(\epsilon^0)$ the homogeneous modes is the expected state $A_0^{(0)} = a/b$ and to $O(\epsilon^{1/2})$ stochastic realizations $x(t)$ correspond to an Ornstein-Uhlenbeck process that will lead to the saturation of the dispersion of the homogeneous mode $A_0(t \gg a) = a/b + \sqrt{\epsilon}x(\infty) + \cdots$, where $x(\infty)$ is a Gaussian random variable. Concerning the unstable mode, up to $O(\epsilon^{1/2})$, the realizations $W(t)$ correspond to an exponentially increasing stochastic process (SP), therefore these realizations will lead the dominant escape processes toward the final attractor of the nonlocal Fisher equation (see Figs. 1 and 2). The distribution for the escape times, i.e., the FPTD $P(t_e)$ to reach a given threshold value $A_e \equiv \Delta u$, can be written, using a nondimensional unit of time $\tau_e = \varphi t_e$, as (see Appendix D and [8,9])

$$P(\tau_e) = \frac{2K}{\mathrm{erf}(K)\sqrt{\pi}} \exp[-\tau_e - K^2\exp(-2\tau_e)],$$
$$K = A_e\sqrt{\frac{\varphi}{\epsilon}}, \quad \tau_e = \varphi t_e. \tag{48}$$

The MFPT is

$$\langle \tau_e \rangle = \int_0^\infty P(\tau_e)d\tau_e \simeq \ln(K) + \frac{E + \ln 4}{2\mathrm{erf}(K)}, \quad K \gg 1, \tag{49}$$

where E is the Euler constant. Note that the general solution of the escape problem (for the supercritical case) has been written in terms of the nondimensional parameter (group) $K = A_e\sqrt{\varphi/\epsilon}$; the group K explicitly depends on the diffusion constant D through the phase parameter $\varphi = -Dk_e^2 - 2aG_e > 0$.

B. Stochastic escape at the critical point $\varphi = 0$

Before going into any mathematical detail we point out that the MCA does not allow us to get, for the critical case, the value of $A_e(t=\infty)$; however the MCA indeed describes very well the growth of the explosive mode $A_e(t<\infty)$ when the perturbation is taken to $O(\epsilon^1)$. The critical case happens when $\varphi = -Dk_e^2 + 2a|G_e| = 0$, therefore from (41)–(44) and (45)–(47) we realize that a drastic change in the short-time evolution of the unstable mode will occur. The important point is therefore to solve properly the unstable escape, which is now controlled by both realizations $W(t)$ and $V(t)$. The solution of $W(t)$ is now a Wiener path. Therefore, if we only take into account corrections to $O(\epsilon^{1/2})$ the MFPT is scaled down as a random-walk process. This perturbation is not enough to characterize the dynamics of the unstable mode $A_e(t)$, therefore we need to go one step further and solve the realizations of the SP $V(t)$. We can also see that to $O(\epsilon^1)$ the stochastic perturbation is nontrivial and with a multiplicative character, therefore we choose from now on, if necessary, the Stratonovich calculus.

For the critical case ($\varphi = 0$) the dynamics up to $O(\epsilon^1)$ are reduced to

$$A_0(t) \Rightarrow \frac{dx}{dt} = -ax(t) + \xi_0(t)$$
$$\Rightarrow \frac{dy}{dt} = -ay(t) - bx(t)^2 - 2bG_eW(t)^2 \qquad (50)$$

and

$$A_e(t) \Rightarrow \frac{dW}{dt} = \xi_e(t)$$
$$\Rightarrow \frac{dV}{dt} = -b(1+2G_e)W(t)x(t), \qquad (51)$$

showing that $A_0(t)$ is dominated by an additive noise, but $A_e(t)$ by a nontrivial multiplicative SP. Note that up to $O(\epsilon^{1/2})$ the escape time is controlled by the Wiener SP $W(t)$, which will not give a good description because the MFPT would be as in a random walk.

Perturbations up to $O(\epsilon^1)$

The homogeneous mode is simple to solve in the spirit of the stochastic path perturbation approach. First we note that for $t \to \infty$ the SP $x(t)$ saturates to its stationary state; therefore we can introduce the notation Ω to characterize the random variable $x(\infty) = \Omega$, which, in addition, is characterized by the normal PDF

$$P(\Omega) = \frac{\exp\left(-\Omega^2/2\sigma_\Omega^2\right)}{\sqrt{2\pi\sigma_\Omega^2}}, \quad \sigma_\Omega^2 = \frac{1}{2a}, \quad \Omega \in (-\infty,\infty). \qquad (52)$$

Using that $x(t)$ is the Ornstein-Uhlenbeck SP and $W(t)$ is the Wiener SP [uncorrelated because they come from stochastic integrals of $\xi_0(t)$ and $\xi_e(t)$, respectively] we could approximate (43), for $at \gg 1$, by

$$\{x(t) \simeq \Omega\} \Rightarrow \frac{dy}{dt} \simeq -ay(t) - b\Omega^2 - 2bG_eW(t)^2. \qquad (53)$$

In this approximation the realization of $y(t)$ can be written in the form

$$y(t) \simeq \frac{-b\Omega^2}{a}(1 - e^{-at}) + 2b|G_e|\Theta(t). \qquad (54)$$

Nevertheless, we do not need to use realizations $y(t)$ to study the escape problem. Note that here $\Theta(t)$ is a non-Gaussian SP characterized by

$$\Theta(t) = \int_0^t e^{-a(t-t')}W(t')^2dt'. \qquad (55)$$

Then all the moments and correlations of the SP $\Theta(t)$ can be calculated using Wiener paths (see Appendix E).

Now we proceed to solve up to $O(\epsilon^1)$ the dynamics of the unstable mode $A_e(t)$. In this case we can approximate (51), for $at \gg 1$, by

$$\{\varphi = 0, x(t) \simeq \Omega\} \Rightarrow \frac{dV}{dt} \simeq -b(1+2G_e)W(t)\Omega. \qquad (56)$$

Thus defining $\beta \equiv b(1+2G_e) > 0$ we can approximate the realization of SP $V(t)$ by

$$V(t) \simeq -\beta\Omega\Lambda(t), \qquad (57)$$

where $\Lambda(t)$ is a Gaussian SP defined in terms of a Wiener integral

$$\Lambda(t) = \int_0^t W(t')dt'. \qquad (58)$$

Thus any realization $V(t)$ is characterized by the Gaussian SP $\Lambda(t)$. In particular, the first and second moments can be calculated straightforwardly (similar calculations are shown in Appendix E)

$$\langle V(t)\rangle = 0,$$
$$\langle V(t)^2\rangle = \beta^2\langle\Omega^2\rangle\int_0^t dt_1\int_0^t dt_2 \min(t_1,t_2) = \frac{\beta^2}{2a}\frac{t^3}{3}. \qquad (59)$$

Therefore, up to $O(\epsilon^1)$ the realizations of $A_0(t)$ and $A_e(t)$ can be analyzed. First we note that $V(t)$ grows faster than $y(t)$, which shows the explosive character of the unstable mode $A_e(t)$ when it is compared with the growth of the homogeneous mode $A_0(t)$. In fact, for the homogeneous mode we get that

$$A_0(t) \simeq b/a + \sqrt{\epsilon}x(t) + \epsilon y(t) + \cdots, \qquad (60)$$

where

$$\langle x(t)\rangle = 0, \quad \langle x(t)x(s)\rangle = \frac{1}{2a}(e^{-a|t-s|} - e^{-a(t+s)}). \qquad (61)$$

In (60) the SP $y(t)$ can be approximated by Eq. (54), thus we can calculate its mean value, etc. (see Appendix E).

For the unstable mode we get

$$A_e(t) \simeq \sqrt{\epsilon}W(t) + \epsilon V(t) + \cdots, \qquad (62)$$

where, for example,

$$\langle W(t)\rangle = 0, \quad \langle W(t)W(s)\rangle = \min\{t,s\}, \qquad (63)$$

$$\langle V(t)\rangle = 0, \quad \sqrt{\langle V(t)^2\rangle} = \sqrt{\frac{\beta^2}{6a}t^3}. \qquad (64)$$

Here the SP $V(t)$ is approximated for $at \gg 1$ by Eq. (57).

From (50) it is possible to see that at short times the SP $y(t)$ decreases, but because $G_e < 0$ the process may grow due to the contribution of the square of the Wiener SP. On the other hand, the evolution of the unstable mode can also be interpreted: At the origin of time $t = 0$ the mode is null and then at short time $A_e(t \approx 0)$ it starts to growth as a Wiener process. After this regime the nonlinear contribution [proportional to $x(t)W(t)$] fluctuates with mean value zero, but grows faster that the Wiener SP [$\sqrt{\langle W(t)^2\rangle} \sim t^{1/2}$ and $\sqrt{\langle V(t)^2\rangle} \sim t^{3/2}$]. We note here that the next order of perturbation $O(\epsilon^{3/2})$ can be analyzed in a similar way, showing in addition much more complex stochastic dynamics that could also be solved, in some approximation, in the context of the stochastic path perturbation approach.

C. Calculation of the MFPT (passage times for the critical case)

Equation (57) characterizes the random escape times t_e; to see this we use the scaling of the Wiener process. First we write a threshold value $V_e \equiv V(t_e)$ in the form

$$V_e = -\beta\Omega\Lambda(t_e), \quad \beta \equiv b(1 + 2G_e). \tag{65}$$

Then, using Wiener paths in (58), we can prove, in the distribution, the following scaling for the SP $\Lambda(t)$:

$$\Lambda(t_e) = \int_0^{t_e} W(t')dt' \doteq t_e^{3/2} \int_0^1 W(s)ds \equiv t_e^{3/2}\Lambda, \tag{66}$$

where $\Lambda \equiv \Lambda(1) = \int_0^1 W(s)ds$ is a random variable characterized by the normal PDF

$$P_\Lambda(\Lambda) = \frac{\exp(-\Lambda^2/2\langle\Lambda^2\rangle)}{\sqrt{2\pi\langle\Lambda^2\rangle}},$$
$$\langle\Lambda^2\rangle = \frac{1}{3}, \quad \Lambda \in (-\infty,\infty). \tag{67}$$

Now using the scaling (66), we can invert (65). This will give a mapping for the random escape times t_e from the set of random variables Ω,Λ:

$$t_e^3 = \left(\frac{V_e}{\beta\Omega\Lambda}\right)^2 = \left(\frac{A_e/\epsilon}{\beta\Omega\Lambda}\right)^2. \tag{68}$$

In the second line we have used Eq. (40), i.e., the multiple-scaling expansion to $O(\epsilon^1)$, so here A_e is a given threshold value $A_e \equiv \Delta u$. Noting that $\{\Omega,\Lambda\}$ are statistically independent random variables and using (67) and (52), we can now calculate the MFPT taking the average of (68),

$$\begin{aligned}\langle t_e\rangle &= \left\langle\left(\frac{A_e/\epsilon}{\beta\Omega\Lambda}\right)^{2/3}\right\rangle_{P_\Lambda P_\Omega}\\ &= \epsilon^{-2/3}\left(\frac{A_e}{\beta}\right)^{2/3}\left\langle\left(\frac{1}{\Omega}\right)^{2/3}\right\rangle_{P_\Omega}\left\langle\left(\frac{1}{\Lambda}\right)^{2/3}\right\rangle_{P_\Lambda}\\ &= \epsilon^{-2/3}\left(\frac{A_e}{b(1+2G_e)}\right)^{2/3}\left(\frac{\Gamma(1/6)}{\sqrt{\pi}2^{1/3}}\right)^2(6a)^{1/3}.\end{aligned} \tag{69}$$

In Table III we show a comparison of the theoretical prediction for the MFPT (69) against numerical simulations using the threshold value $\Delta u = 0.275$ (see Appendix B and Fig. 1). In Fig. 5 we present a plot showing the predicted scaling with the noise intensity ϵ.

TABLE III. Mean first-passage time.

Noise intensity	Theoretical MFPT	Numerical MFPT
$\epsilon = 10^{-3}$	561	544.2
$\epsilon = 5\times10^{-3}$	192	222.6
$\epsilon = 10^{-2}$	120	128.5
$\epsilon = 5\times10^{-2}$	41	15.04
$\epsilon = 10^{-1}$	26	3.77

We note that having worked the stochastic perturbation up to $O(\epsilon^1)$ has modified the scaling of the MFPT with the noise intensity, i.e., now we get $\langle t_e\rangle \sim \epsilon^{-2/3}$, which is slower than the scaling that we would have obtained working up to $O(\epsilon^{1/2})$, i.e., a random-walk process predicting the scaling $\langle t_e\rangle \sim (A_e/\sqrt{\epsilon})^2 \propto \epsilon^{-1}$. Comparing the behavior (69) with the one for the supercritical case (49), $\langle t_e\rangle \sim \ln(\frac{1}{\epsilon})$, we can see the occurrence of a critical slowing down when the phase factor reaches the null value $\varphi = 0$.

D. Calculation of the FPTD for the critical case

A crude approximation for the FPTD can be calculated from (68) when this map is written in the form of a random variable transformation law from the set of random variables $\{\Omega,\Lambda\}$ to the random time t_e, i.e.,

$$\begin{aligned}P(t_e) &= 2\iint_0^\infty P_\Omega(\Omega)P_\Lambda(\Lambda)\delta\left(t_e - \left(\frac{A_e/\epsilon}{\beta\Omega\Lambda}\right)^{2/3}\right)d\Omega d\Lambda,\\ &\quad t_e \geqslant 0\\ &= 2\iint_0^\infty P_\Omega(\Omega)P_\Lambda(\Lambda)\frac{\delta(\Omega-\Omega')}{|J|}d\Omega d\Lambda,\end{aligned}$$

where $|J|$ is the Jacobian of the transformation and $\Omega' = A_e/t_e^{3/2}\epsilon\beta\Lambda$ is the root of the mapping (68). Performing the

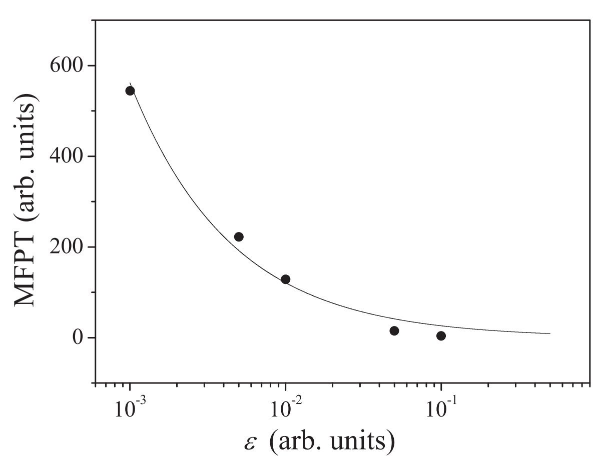

FIG. 5. The MFPT for the critical case from Eq. (69) as a function of the noise intensity ϵ. The values of the parameters that we have used are shown in Tables I and II; $A_e = \Delta u = 0.275$. The line is the predicted scaling law $\epsilon^{-2/3}$.

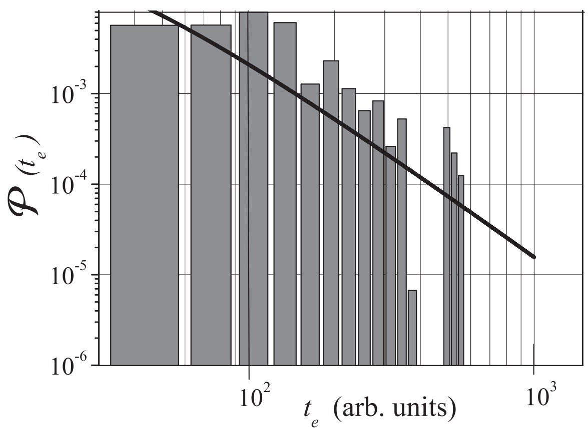

FIG. 6. A log-log plot of the escape time probability distribution (for the critical case) from Eq. (70) as a function of time t_e. The values of the parameters that we have used are shown in Tables I and II; $A_e = \Delta u = 0.275$ and $\epsilon = 10^{-2}$. The histogram from numerical simulations is also included for comparison with the predicted long-time tail.

algebra, we arrive at

$$\begin{aligned} P(t_e) &= 2\int_0^\infty P_\Omega(\Omega')P_\Lambda(\Lambda)\frac{d\Lambda}{|J|} \\ &= \frac{6A_e}{\epsilon\beta t_e^{5/2}}\sqrt{\frac{3a}{2\pi^2}}K_0\left[\frac{A_e\sqrt{6a}}{\epsilon\beta t_e^{3/2}}\right], \\ \beta &\equiv b(1+2G_e), \end{aligned} \tag{70}$$

where $K_0[z]$ is the K Bessel function of order 0. Using the asymptotic result $K_0[z \to 0] \to \ln(2/z) - E$, where E is the Euler constant [30], we get the long-time tail in the asymptotic behavior of the FPTD

$$P(t_e \to \infty) \propto \frac{\ln t_e}{t_e^{5/2}}. \tag{71}$$

The map (68) is an approximation for $at \gg 1$ and small noise. In fact, this mapping gives a quite good result for the calculation of the MFPT at the critical point, as shown in Table III and Fig. 5 [the long tail (71) dominates this calculation]. Nevertheless, we cannot expect that the FPTD given by (70) would be a good description at short times (see the histogram in Fig. 3). We also note that the escape time at the critical point does not depend explicitly on the value of the diffusion constant D (this is so because the phase φ is null). Figure 6 shows a log-log plot of the FPTD (70) to emphasize its long-time tail; the agreement with the numerical simulations (using 5×10^4 realizations) can also be seen.

To end this section let us note that the FPTD $P(t_e)$ can be written using a nondimensional unit of time in the form

$$\begin{aligned} P(\tau_e) &= \frac{3Q}{\pi\tau_e^{5/2}}K_0\left[\frac{Q}{\tau_e^{3/2}}\right], \\ Q &\equiv \frac{A_e\sqrt{6a\beta}}{\epsilon}, \quad \tau_e = \beta t_e. \end{aligned} \tag{72}$$

Thus, up to a perturbation of $O(\epsilon^1)$ the general solution for the escape problem (at the critical point) can be written in terms of a nondimensional group Q that depends on the nonlinear parameter b. We note this result against the FPTD in the supercritical case $\varphi > 0$; there the distribution does not depend on the parameter b because the instability is linear. On the other hand, as we pointed out before, in the supercritical case the MCA does indeed allow the calculation of the stationary value $A_e(\infty)$, a situation that cannot be achieved in the critical case $\varphi = 0$ [see Eqs. (35) and (36)]. Therefore, our solution (72) for the FPTD in the critical case must be handled using A_e as a threshold value Δu. We show in Appendix B that only by going beyond the MCA is it possible to find the stationary state $A_e(\infty)$. We made numerical simulations (in real space-time) for the histogram of the escape times of the field $u(x,t)$ through a given threshold value $\Delta u = 0.275$, using the time evolution of the nonlocal Fisher equation (1). In Table III and Fig. 5 we show the agreement with the theoretical prediction of the MFPT vs noise intensity and in Fig. 6 we show the agreement with the predicted long-time tail of the FPTD.

In addition, from the nondimensional solution presented in Eq. (72) it is simple to study the dispersion of the random escape times. In fact, we can calculate $\sigma^2 \equiv \langle\tau_e^2\rangle - \langle\tau_e\rangle^2$; then it is possible to show that this dispersion grows as a function of the universal parameter Q. A quantity that is more relevant for this statistical analysis is the relative dispersion $\sigma/\langle\tau_e\rangle$; this statistical indicator is bounded as a function of Q. This result indicates that the MFPT gives a good description of the pattern formation (for the critical case) as a function of the universal parameter Q.

VII. CONCLUSION

In this work we have presented a general approach to tackle the problem of the characterization of the mean first-passage time from an initial homogeneous unstable state towards a final patterned stable attractor. In particular, we applied this general approach when the evolution is associated with stochastic integro-differential spatial dynamics as in the Fisher-like equation. The theory is based on the technique of scaling down Wiener integrals (i.e., the stochastic path perturbation approach) with the additional implementation of the minimum coupling approximation in the context of the Fourier analysis. This approximation allowed us to study analytically the random escape times from an initial unstable state.

We have introduced a stochastic multiple-scale analysis that is a fundamental tool that allow us to undertake the random escape problem by introducing perturbations to any nonlinear instability. The critical case ($\varphi = 0$), when the phase of the Fourier perturbation is zero, has been solved analytically and compared with numerical simulations of the field $u(x,t)$ in real space-time. Despite the many approximations that we have introduced, the predictions for the MFPT are in good agreement with the numerical simulations. In addition, we have shown the existence of a universal (group) parameter Q that characterizes the FPTD in a nondimensional unit of time $\tau_e = \beta t_e$. This universal parameter $Q \equiv \frac{A_e}{\epsilon}\sqrt{6a\beta}$ is different from the universal (group) parameter $K \equiv A_e\sqrt{\varphi/\epsilon}$ for the supercritical case [compare Eqs. (72) and (48)].

In addition to the stochastic analysis that we have presented to describe the pattern formation in the nonlocal Fisher equation (when the fully populated state turns out to be unstable due to the nonlocal interaction) we have presented an exact deterministic analysis to study the bifurcation point for the stationary state $u_{SS} = a/b$ (i.e., we found a minimum value for the range $w_{\min} = \sqrt{-3\kappa^2/\cos\kappa}\sqrt{\frac{D}{a}}$). Also, the occurrence of wave fronts between the unpopulated and the fully populated states has been studied. In particular, we carried out an asymptotic perturbation analysis to study the critical velocity of the front $c_{\min} = 2\sqrt{aD} + O(w^4)$, when the range of the nonlocal kernel is small (using a square kernel function). Another model of kernels would allow a simpler analysis of the front propagation.

To end this section we comment that if the noise would appear in some physical parameter, for example, if the growth rate changes in the form $a \to a + \xi(x,t)$, the stochastic problem turns out to be of multiplicative character, which is different from the equation (1) that we have worked out in the present paper. These types of problems can also be properly tackled using the present stochastic multiscale expansion. We are confident that our theoretical approach to solve the mean first-passage time may help in the general understanding of the pattern formation in complex systems where the nonlocal interaction (considering a range of interaction) plays an important role in the description of real systems. In addition, the present stochastic multiple-scale approach may also help to solve a quite different but related problem: the study of zero-dimensional dynamical systems with distributed time delay. These types of situations can be of interest in the study of pattern formation in biological models [28,31].

ACKNOWLEDGMENT

M.A.F. thanks CONICYT, Anillo en Complejidad Social, SOC1101, FONDECYT 1140278.

APPENDIX A: BIFURCATION POINT FOR THE STEADY STATE $u_{SS} = a/b$

The bifurcation point $w_{\min}$ associated with the steady state $u_{SS} = a/b$ can be calculated from Eqs. (6) and (7) to obtain

$$\varphi(k_c) = -Dk_c^2 - a\frac{\sin k_c w}{k_c w} = 0, \tag{A1}$$

$$\varphi'(k_c) = -2Dk_c - a\left(\frac{\cos k_c w}{k_c} - \frac{\sin k_c w}{k_c^2 w}\right) = 0. \tag{A2}$$

Solving $\sin k_c w/k_c^2 w$ from Eq. (A1) and introducing this expression in Eq. (A2) we get

$$\frac{Dk_c^2}{a} = -\frac{1}{3}\cos k_c w; \tag{A3}$$

however, from Eq. (A1) we can write

$$\frac{Dk_c^2}{a} = -\frac{\sin k_c w}{k_c w}. \tag{A4}$$

By defining $k_c w \equiv \kappa$ and comparing Eqs. (A3) and (A4) the following condition should be fulfilled:

$$3\tan\kappa = \kappa, \quad \kappa \in (0,2\pi).$$

Thus, from Eq. (A3) we can write

$$\frac{D\kappa^2}{aw^2} = -\frac{1}{3}\cos\kappa,$$

from which the bifurcation point is characterized by

$$w_{\min} = \sqrt{-3\kappa^2/\cos\kappa}\sqrt{\frac{D}{a}}. \tag{A5}$$

In nondimensional units (see Sec. III B) there is only one free parameter w, so the bifurcation is characterized by a point: the minimum value of the interaction range $w_{\min} = \sqrt{-3\kappa^2/\cos\kappa} = 9.1760\ldots$. For values in the range $w > w_{\min}$ the dynamics of the system are of the supercritical case.

APPENDIX B: UPPER BOUND OF $A_e(\infty)$ AT THE CRITICAL POINT

We have already commented that at the critical point $\varphi = 0$, the MCA does not allow us to calculate the stationary state of the amplitude $A_e(\infty)$. Here we show that only by going beyond the MCA could we get a value for this amplitude. This can be done by analyzing the full Fourier set of deterministic equations (19) under an effective approach and invoking a small-amplitude approximation.

In analogy with the deterministic structure of the set of equations (24)–(26), we assume here that there is only one unstable mode k_e. Then we can characterize the stationary amplitudes by the set of equations (in the symmetric case $A_e = A_{-e}$)

$$0 = (a - bA_0)A_0 - 2b\left[2A_e^2 G_e + X_e\right], \tag{B1}$$

$$0 = [a(e) - bA_0(1 + 2G_e)]A_e - 2bY_e, \tag{B2}$$

$$0 = [a(m) - bA_0(1+2G_m)]A_m - 2bY_m, \quad m \neq \{0,e\}, \tag{B3}$$

where X_e, Y_e, and Y_m are given by

$$X_e \equiv \sum_{l>0,l\neq e} 2A_l^2 G_l > 0, \tag{B4}$$

$$Y_e \equiv \sum_{l\neq\{0,e\}} A_{e-l}A_l G_l, \tag{B5}$$

$$Y_m \equiv \sum_{l\neq\{0,m\}} A_{m-l}A_l G_l. \tag{B6}$$

Noting that $G_e < 0$ and $G_l > 0\,\forall l \neq \{0,\pm e\}$, we can find the dominant solutions of Eqs. (B1)–(B3) in the following way. Apart from any possible (but small) solution $A_m(\infty)$ from (B3), at the critical point $[a(e) - b(\frac{a}{b})(1 + 2G_e)] = 0$ the system of equations (B1)–(B3) has a solution if

$$A_0 = a/b,$$
$$2A_e^2 = -X_e/G_e,$$
$$A_m \sim 0,$$
$$Y_m \sim 0,$$
$$Y_e = 0.$$

The last two conditions can be accepted by invoking a sort of null compensation in the sum of small-amplitude modes. Then, from (B1), noting that $G_e < 0$, we arrive at the important conclusion

$$A_0|_{\varphi=0} = a/b, \tag{B7}$$

$$A_e|_{\varphi=0} = \sqrt{\frac{\sum_{l>0,l\neq e} A_l^2 G_l}{|G_e|}}. \tag{B8}$$

From this result we can see that the value of $A_e(\infty)$ is beyond the MCA because it is of $O(X_e)$, as we had pointed out before.

An upper bound for A_e can be obtained by using Parseval's identity. Let $u_{SS}(x)$ be a inhomogeneous deterministic stationary state of the Fisher nonlocal equation (1),

$$u_{SS}(x) = u(x,t=\infty) = A_0 + \sum_{n=-\infty}^{\infty} A_n \exp(ik_n x) = A_0 + \sum_{j=1}^{\infty} 2A_j \cos(k_j x). \tag{B9}$$

Note that the cosine expansion is not really true for $u(x,t)$ during the transition when there is noise. In the stationary state we can write

$$C \equiv \frac{1}{2}\int_{-1}^{1} u_{SS}(x)^2 dx = \sum_{j=-\infty}^{\infty} A_j^2 = A_0^2 + 2A_e^2 + \sum_{j>0, j\neq e} 2A_j^2. \tag{B10}$$

From Eq. (B8) and because in the symmetric case $0 < G_j < 1$ for $j \neq e$, we get

$$A_e^2 |G_e| = \sum_{l>0, l\neq e} A_l^2 G_l \leqslant \sum_{l>0, l\neq e} A_l^2 = \left(C - A_0^2 - 2A_e^2\right)/2.$$

Then we finally arrive at the upper bound

$$A_e \leqslant \sqrt{\frac{C - A_0^2}{2(1+|G_e|)}} \simeq \sqrt{\frac{C-(a/b)^2}{2(1+|G_e|)}}. \tag{B11}$$

Thus, if we calculate C numerically from Eq. (1) with $\epsilon = 0$, the inequality (B11) provides the upper bound we were seeking for the amplitude $A_e(\infty)$ at the critical point. We have measured numerically C from the stationary state of the deterministic Fisher nonlocal equation (see Fig. 2). For the critical parameters that we have used (see Table I and II) we get $C \simeq 1.05$, therefore from (B11) we get $2A_e \leqslant 0.300$ [the factor 2 can be considered a threshold value from a cosinelike expansion (B9)]. Then, in our simulations the MFPT was calculated using the threshold value $\Delta u \equiv [u(x,t_e)_{\max} - u(x,t_e)_{\min}]/2 = 0.275$.

APPENDIX C: THE MCA FOR THE CASE OF TWO UNSTABLE FOURIER MODES

In the symmetric case $G_n = G_{-n}$, considering a situation when there are only two unstable modes $A_e(t) = A_{-e}(t)$ and $A_u(t) = A_{-u}(t)$ in (19) and the rest of the modes $A_n\ \forall n \neq \{e,u,0\}$ are of small amplitude, we can write a Fourier coupled system of equations in the form

$$\frac{dA_0}{dt} = (a - bA_0)A_0 - 2b\left[2A_e^2 G_e + 2A_u^2 G_u + B_e\right], \tag{C1}$$

$$\frac{dA_e}{dt} = [a(e) - bA_0(1+2G_e)]A_e - 2b[A_{e-u}A_u G_u + E_e], \tag{C2}$$

$$\frac{dA_u}{dt} = [a(u) - bA_0(1+2G_u)]A_u - 2b[A_{u-e}A_e G_e + E_u], \tag{C3}$$

where $[a(e) - bA_0(1+2G_e)]_{A_0=a/b} \equiv \varphi_e \geqslant 0$ and $[a(u) - bA_0(1+2G_u)]_{A_0=a/b} \equiv \varphi_u \geqslant 0$ are the Fourier phase factors of the unstable modes. On the other hand,

$$B_e = \sum_{j>0, \{j\neq e,u\}} 2A_j^2 G_j > 0,$$

$$E_e = \sum_{j\neq\{0,e,u\}} A_{e-j} A_j G_j,$$

$$E_u = \sum_{j\neq\{0,e,u\}} A_{u-j} A_j G_j.$$

Therefore, because only G_e and G_u are negative we can neglect all terms proportional to G_j with $j \neq \{e,u\}$ in (C1)–(C3). Thus we can conclude that this set of equations represents the MCA for the case when there are two unstable modes. This MCA predicts a nontrivial interaction between the modes A_e and A_u that must be worked out with some effective approximation for the small amplitude $A_{|e-u|}$.

APPENDIX D: CALCULATION OF THE MFPT IN THE SUPERCRITICAL CASE

Using that $\varphi > 0$, from Eqs. (42) and (45) we can write both stochastic realizations in the form

$$x(t) = \int_0^t \exp[-a(t-t')]\xi_0(t')dt', \quad x(0) = 0, \quad t \geqslant 0 \tag{D1}$$

$$W(t) = \int_0^t \exp[\varphi(t-t')]\xi_e(t')dt', \quad W(0) = 0, \quad t \geqslant 0. \tag{D2}$$

From expression (D1) we note that for $t \to \infty$ the SP $x(t)$ saturates to its stationary state. Therefore, we can introduce the notation Ω to characterize the random variable $x(\infty) = \Omega$, which in addition can be seen to be characterized by the normal PDF

$$P(\Omega) = \frac{\exp\left(-\Omega^2/2\sigma_\Omega^2\right)}{\sqrt{2\pi\sigma_\Omega^2}}, \quad \sigma_\Omega^2 = \frac{1}{2a}, \quad \Omega \in (-\infty,\infty). \tag{D3}$$

On the other hand, from (D2), the SP $W(t)$ can be written in the form

$$W(t) = e^{\varphi t}\eta(t), \tag{D4}$$

where the SP $\eta(t)$ fulfills the stochastic differential equation

$$\frac{d\eta}{dt} = e^{-\varphi t}\xi_e(t), \quad \eta(0) = 0, \quad t \geqslant 0.$$

In addition, it is possible to see that the SP $\eta(t)$ also saturates for times $t \gg \varphi^{-1}$. Then the random variable $\eta(\infty) \equiv \eta$ is characterized by the normal PDF

$$P(\eta) = \frac{\exp\left(-\eta^2/2\sigma_\eta^2\right)}{\sqrt{2\pi\sigma_\eta^2}}, \quad \sigma_\eta^2 = \frac{1}{2\varphi}, \quad \eta \in (-\infty,\infty) \equiv D_\eta. \tag{D5}$$

Approximating $\eta(t) \sim \eta(\infty)$ in Eq. (D4), we can extract the escape times t_e by inverting a random mapping, i.e., we can study the random escape times t_e from a random transformation law $\eta \to t_e$ (into a suitable support to ensure $t_e \geqslant 0$). To see this we first define t_e as the time it takes for the stochastic process $W(t)$ to reach a threshold value W_e. Then we approximate Eq. (D4) by

$$W_e^2 = W(t_e)^2 \simeq e^{2\varphi t_e}\eta(\infty)^2 = \eta^2 \exp(2\varphi t_e). \tag{D6}$$

Now we can solve from (D6) the random escape time as a function of the threshold W_e, η, and φ,

$$t_e = \frac{1}{2\varphi} \ln \left(\frac{W_e}{\eta}\right)^2, \quad \frac{W_e}{\eta} \geqslant 1,$$

where η is a normal distributed random variable [see Eq. (D5)]. Now using the scaling (40) we write $W_e = A_e/\sqrt{\epsilon}$. Then the random mapping we were looking for is

$$t_e = \frac{1}{2\varphi} \ln \left(\frac{A_e^2}{\eta^2 \epsilon}\right). \tag{D7}$$

Here A_e is a threshold value used to characterize the pattern formation, i.e., the transition from $A_e(t=0) \sim 0$ to the patterned state $A_e(t_e) \sim O(1)$. Finally, the PDF for the escape times, i.e., the FPTD $P(t_e)$, can be obtained from the theorem of the transformation of random variables

$$P(t_e) = \int \delta\left(t_e - \frac{1}{2\varphi} \ln \frac{A_e^2}{\eta^2 \epsilon}\right) P(\eta) d\eta, \quad t_e \geqslant 0. \tag{D8}$$

After some algebra we get (48). We can calculate the MFPT by taking the average of Eq. (D7) (or from the first moment of the FPTD) to obtain

$$\langle t_e \rangle = \frac{1}{2\varphi} \left\langle \ln \frac{A_e^2}{\eta^2 \epsilon} \right\rangle.$$

Thus using a nondimensional time $\tau_e = \varphi t_e$ we get Eq. (49).

APPENDIX E: CALCULATION OF MOMENTS OF THE PROCESS $\Theta(t)$

To calculate the first moment of the non-Gaussian SP $\Theta(t) = \int_0^t e^{-a(t-t')} W(t')^2 dt'$ we use that for the Wiener SP we know that $\langle W(t)^2 \rangle = t$, Then

$$\langle \Theta(t) \rangle = \int_0^t e^{-a(t-t')} \langle W(t')^2 \rangle dt' = \int_0^t e^{-a(t-t')} t' dt'$$
$$= \frac{1}{a}\left(t - \frac{1}{a}\right) - \frac{e^{-at}}{a^2}.$$

Therefore, in the long-time limit we get ($at \gg 1$)

$$\langle \Theta(t) \rangle \to t/a.$$

To calculate the second moment of the SP $\Theta(t)$ we use Novikov's theorem [1,25,26] for the Wiener SP

$$\langle W(t_1)W(t_2)W(t_3)W(t_4)\rangle = \min(t_1,t_2)\min(t_3,t_4) + \min(t_1,t_3)\min(t_2,t_4) + \min(t_1,t_4)\min(t_2,t_3).$$

Then we can write $\langle W(t_1')^2 W(t_2')^2 \rangle = (t_1' t_2' + 2[\min\{t_1', t_1'\}])$ and so we get

$$\langle \Theta(t)^2 \rangle = \int_0^t e^{-a(t-t_1')} dt_1' \int_0^t e^{-a(t-t_2')} \langle W(t_1')^2 W(t_2')^2 \rangle dt_2'$$
$$= \int_0^t e^{-a(t-t_1')} dt_1' \int_0^t e^{-a(t-t_2')} (t_1' t_2' + 2[\min\{t_1', t_1'\}]) dt_2'$$
$$= \frac{1}{a^4}\{7 + e^{-2at} - 8e^{-at} + 2at(-3 + at).$$
$$+ e^{-2at}[1 + e^{at}(-1 + at)]^2\}.$$

Therefore, in the long-time limit we get (for $at \gg 1$)

$$\langle \Theta(t)^2 \rangle \to 3(t/a)^2.$$

[1] N. G. van Kampen, *Stochastic Processes in Physics and Chemistry*, 2nd ed. (North-Holland, Amsterdam, 1992).

[2] P. Colet, F. De Pasquale, M. O. Cáceres, and M. San Miguel, Phys. Rev. A **41**, 1901 (1990).

[3] P. Colet, F. De Pasquale, and M. San Miguel, Phys. Rev. A **43**, 5296 (1991).

[4] J. M. Sancho and M. San Miguel, Phys. Rev. A **39**, 2722 (1989).

[5] M. O. Cáceres, J. Stat. Phys. **132**, 487 (2008).

[6] M. O. Cáceres, J. Stat. Phys. **156**, 94 (2014).

[7] M. O. Cáceres and M. A. Fuentes, J. Phys. A: Math. Gen. **32**, 3209 (1999).

[8] M. A. Fuentes and M. O. Cáceres, Math. Model. Nat. Phenom. **10**, 48 (2015).

[9] M. A. Fuentes and M. O. Cáceres, Cent. Eur. J. Phys. **11**, 1623 (2013).

[10] A. Mogilner and L. Edelstein-Keshet, J. Math. Biol. **38**, 534 (1999); A. Mogilner, L. Edelstein-Keshet, L. Bent, and A. Spiros, *ibid.* **47**, 353 (2003).

[11] J. D. Murray, *Mathematical Biology*, 3rd ed. (Springer, Berlin, 2007), Vols. 1 and 2.

[12] M. A. Fuentes, M. N. Kuperman, and V. M. Kenkre, Phys. Rev. Lett. **91**, 158104 (2003).

[13] M. A. Fuentes, M. N. Kuperman, and V. M. Kenkre, J. Phys. Chem. B **108**, 10505 (2004).

[14] E. Ben-Jacob, I. Cohen, and H. Levine, Adv. Phys. **49**, 395 (2000).

[15] M. G. Clerc, D. Escaff, and V. M. Kenkre, Phys. Rev. E **72**, 056217 (2005); **82**, 036210 (2010).

[16] I. Demin and V. Volpert, Math. Model. Nat. Phenom. **5**, 80 (2010).

[17] B. L. Segal, V. A. Volpert, and A. Bayliss, Physica D **253**, 12 (2013).

[18] P. Couteron, F. Anthelme, M. Clerc, D. Escaff, C. Fernandez-Oto, and M. Tlidi, Philos. Trans. R. Soc. London Ser. A **372**, 0102 (2014).

[19] C. Fernandez-Oto, M. G. Clerc, D. Escaff, and M Tlidi, Phys. Rev. Lett. **110**, 174101 (2013).

[20] P. C. Bressloff and M. A. Webber, SIAM J. Appl. Dyn. Syst. **11**, 708 (2012).

[21] C. Kuehn and M. G. Riedler, J. Math. Neurosci. **4**, 1 (2014).

[22] V. Volterra, Variazioni e fluttuazioni del numero d'individui in specie animali conciventi [Variations and fluctuations of the number of individuals in animal species living together],

Memoria della R. Accademia Nazionale dei Lincei, Ser. VI 2, pp. 31–113 [English translation: R. Chapman, *Animal Ecology* (McGraw Hill, New York, 1931), pp. 409–448].

[23] R. A. Fisher, Ann. Eugen. London **7**, 355 (1937).

[24] G. Agez, M. G. Clerc, and E. Louvergneaux, Phys. Rev. E **77**, 026218 (2008).

[25] M. O. Cáceres, *Elementos de Estadistica de no Equilibrio y sus Aplicaciones al Transporte en Medios Desordenados* (Reverté, Barcelona, 2003).

[26] J. Garcia-Ojalvo and J. M. Sancho, *Noise in Spatially Extended Systems* (Springer, Berlin, 2010).

[27] A. Kolmogorov, I. Petrovsky, and N. Piscounov, Moscow Univ. Bull. Math. **1**, 1 (1933).

[28] M. O. Cáceres, Phys. Rev. E **90**, 022137 (2014).

[29] M. O. Cáceres and C. D. Rojas R., Physica A **409**, 61 (2014).

[30] M. Abramowitz and I. A. Stegun, *Handbook of Mathematical Functions* (Dover Publication, New York, 1995).

[31] S. Gonçalves, G. Abramson, and M. F. C. Gomes, Eur. Phys. J. B **81**, 363 (2011).